Finite Element Analysis of Reinforced Concrete Coupling Beams

Bambang Budiono, Nyoman Triani Herlina Dewi & Erwin Lim*

Departement of Civil Engineering, Faculty of Civil and Environmental Engineering, Institut Teknologi Bandung, Jalan Ganesha 10, Bandung 40132, Indonesia
*E-mail: erwinlim@si.itb.ac.id

Abstract. The use of reinforced concrete coupling beams in high-rise buildings is popular, especially in seismic prone areas. The modeling of a reinforced concrete coupling beam in a commercial structural analysis software is usually simplified to a line element or a compound of concrete and steel rebar as fiber element. Hence, the analysis of the simplified model cannot capture the overall hysteretic behavior of the element. Moreover, the simplified model is also limited in its capacity to estimate the shear strength contributed by the concrete and diagonal bars, if any, respectively. This study used an advanced finite element analysis package to simulate the cyclic behavior of four coupling beam specimens available in the database. The results show that the hysteretic loop predicted by the finite element analysis tends to overestimate the maximum lateral load capacity. On the other hand, analytical evaluation of the shear strength contributed by concrete and diagonal bars showed good agreement with the test results.

Keywords: *cyclic loading; finite element analysis; reinforced concrete coupling beam; seismic behavior; shear strength.*

1 Introduction

The use of shear walls with coupling beams is popular in high-rise buildings located in seismic prone areas as they provide not only higher stiffness but also better deformability. However, the nonlinear modeling of a reinforced coupling beam is limited to the criteria specified in the ACI 318-14 [1] and ASCE 41-17 [2]. Especially for coupling beams with a diagonal reinforcement layout, their strength is only contributed by the yielding strength of the diagonal bars as expressed in Eq. (1):

$$V_{n,ACI} = 2 \times A_{vd} \times f_y \times \sin\alpha \tag{1}$$

where $V_{n,ACI}$ is the shear strength of a diagonally reinforced coupling beam, A_{vd} is the area of a single group of diagonal bars, f_y is the yield strength of the diagonal bars, and α is the angle between the beam longitudinal axis and the diagonal bars. Previous research [3,4] has pointed out that Eq. (1)

Received January 23rd, 2019,Revised July 22nd, 2019, Accepted for publication October 17th, 2019.
 ISSN: 2337-5779, DOI: 10.5614/j.eng.technol.sci.2019.51.6.2

underestimates the shear strength of a coupling beam with diagonal layout. As a consequence, if a designer strictly follows Eq. (1), it will result in an abundant amount of diagonal bars, which may cause construction difficulties. This has led to the development of other coupling beam systems, such as steel coupling beams embedded in the shear wall [5], or reinforced concrete coupling beams with double beams [6]. However, the disadvantage of using diagonally reinforced coupling beams can be alleviated by including the contribution of the concrete. It has been shown [3,4] that the amount of diagonal bars can be reduced without significantly affecting the seismic behavior. A similar concept of including the concrete contribution has also been suggested by other researchers [7].

The currently available rational models to evaluate the strength of a reinforced concrete coupling beam are mainly limited to the use of the strut-and-tie model [3,4] and modified compression field theory [7]. Using these two models, the concrete and diagonal bar contribution can be well distinguished. However, one should be aware that some assumptions were made when these models were developed. Therefore, it was interesting to analytically investigate the seismic behavior of coupling beams using advanced finite element modeling. Lately, advanced finite element modeling has been shown to be able to successfully simulate the cyclic behavior of reinforced concrete elements [8,9]. Although some limitations may occur, it was expected that this finite element analysis could produce a better understanding of the overall performance of the beams as well as to investigate the contribution of the concrete and diagonal bars on the total shear strength.

In this study, a total of four specimens with span to depth ratio equals 2 and 3, each with and without presence of diagonal bars, were evaluated using the finite element analysis. The analytical results such as hysteretic loops, crack patterns, etc. were compared to the test results.

2 Finite Element Modeling

2.1 Modeled Specimens

In total, this study evaluated four reinforced concrete coupling beam specimens, as shown in Figure 1. Two of these specimens possessed span-to-depth ratio equal to 2.0, and the other two possessed span-to-depth ratio equal to 3.0. For each span-to-depth ratio, one specimen was a conventionally reinforced specimen (Spec. 2-C and Spec. 3-C), while another one was reinforced with a partial amount of diagonal reinforcement (Spec. 2-PD and Spec. 3-PD). The material properties of the four specimens are presented in Table 1.

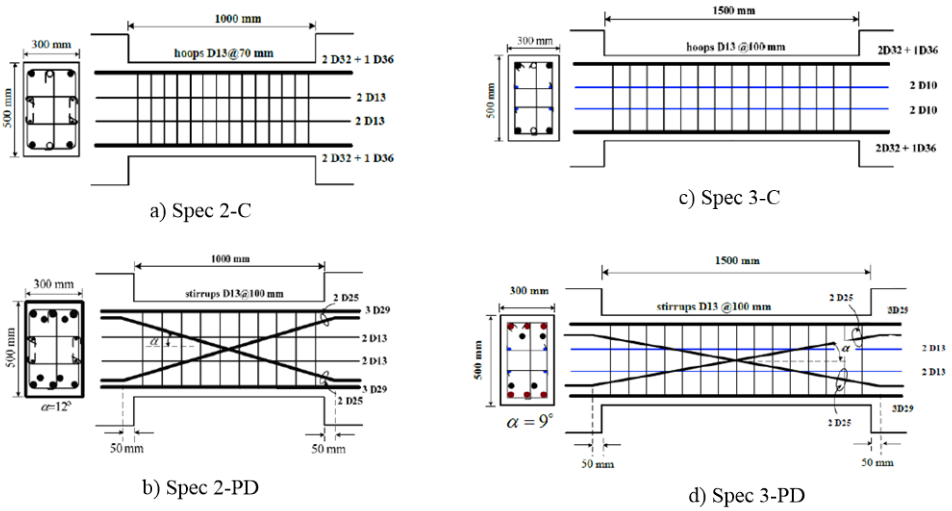

Figure 1 Detailing of the specimens [10].

Table 1 Material properties.

Spec.	f'_c [MPa]	f_y [MPa]					
		D10	D13	D25	D29	D32	D36
2-C	52.2	-	502	-	-	450	448
2-PD	45.1	-	437	461	487	-	-
3-C	47.9	470	441	-	-	465	470
3-PD	52.4	-	502	461	466	-	-

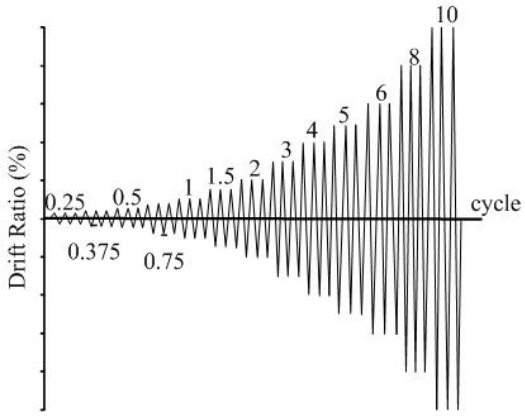

Figure 2 Loading protocol for the experimental test [11].

The four specimens underwent reversed cyclic loading following the displacement loading protocol (Figure 2) specified in ACI 374 [11], with the hysteretic loops presented in Figure 3. The other details, such as crack patterns, test observation, and strain gage measurement, can be found elsewhere [10].

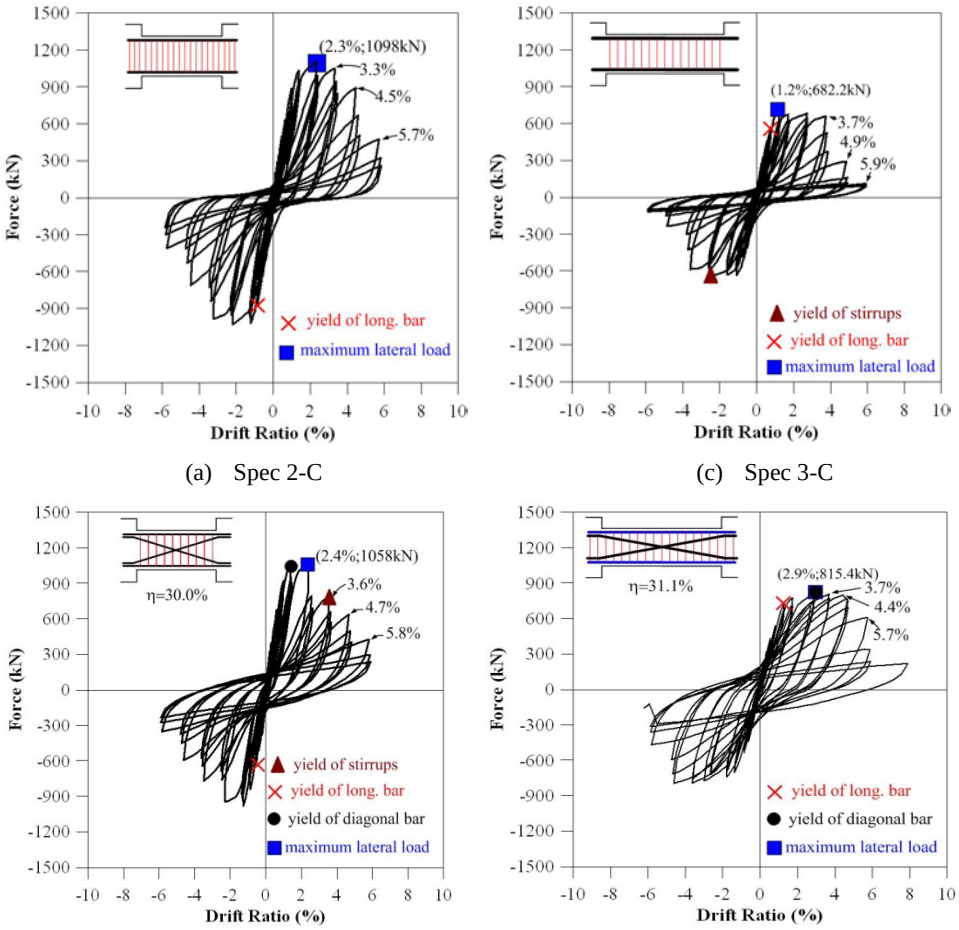

(a) Spec 2-C (c) Spec 3-C

(b) Spec 2-PD (d) Spec 3-PD

Figure 3 Hysteretic loops [10].

2.2 Finite Element Model

ANSYS, a commercial finite element software program, was used to model and analyze the behavior of the four specimens. The concrete material was modeled using SOLID65, which is able to simulate its tensile, crushing, creep, and plastic behavior. The reinforcement bar was modeled as LINK180, while the steel properties used multi-linear kinematic hardening (MKIN), which allows

for Bauschinger's effect. The typical models for specimens reinforced with conventional and partial diagonal layout are presented in Figure 4.

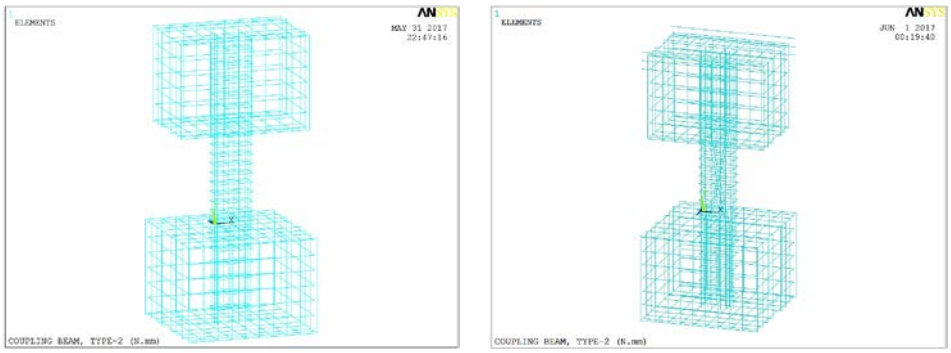

Figure 4 ANSYS model.

Reversed cyclic loading was then applied to each of the specimens following the displacement protocol shown in Figure 5. It is worth noting that the loading protocol assigned in the modeling was slightly different from that in the laboratory. In the modeling, one cycle was applied for each drift ratio, whereas in the laboratory, three cycles were applied. A cycle of up to 3% drift ratio is considered acceptable.

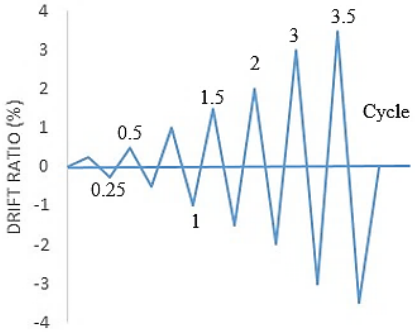

Figure 5 Loading protocol for ANSYS.

3 Experimental Verification and Discussions

3.1 Comparisons of Hysteretic Loops

The hysteretic loops obtained from ANSYS were plotted against those obtained from experimental study for Specimens 2-C, 2-PD, 3-C, and 3-PD in Figures. 6(a)-(d), respectively. To provide comparisons on the same basis, the hysteretic

loops obtained from the experimental study are only presented up to the drift ratio analyzed in ANSYS, i.e. 3%. Lateral force at drift ratios of 1%, 2%, and 3% in both positive and negative directions are presented in Table 2 for comparison purposes. Table 2 also presents the failure modes observed from the test, i.e. flexural shear (FS), shear (S), flexural shear (FS), and flexural shear (FS) for Spec. 2-C, 2-PD, 3-C, and 3-PD, respectively.

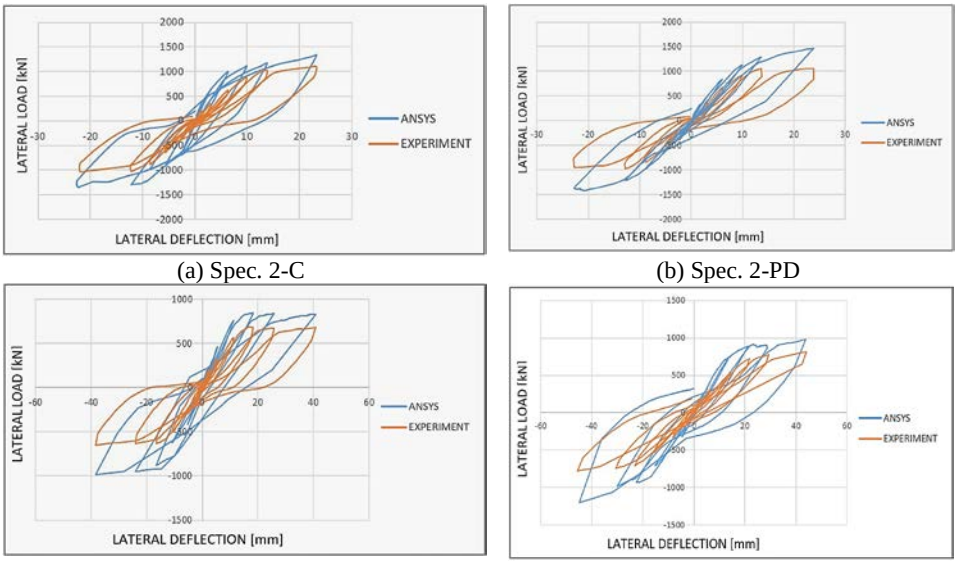

(a) Spec. 2-C (b) Spec. 2-PD

(c) Spec. 3-C (d) Spec. 3-PD

Figure 6 Comparison of hysteretic loops.

Table 2 Comparison between test results and calculated results.

Spec.	DR	Test Result			Calculated Result (ANSYS)			
		Lateral force P[kN]		Failure Mode	Lateral force P[kN]		$V_{n,proposed}$ [kN]	Failure Mode
		Pos.	Neg.		Pos.	Neg.		
2-C	± 1%	626.8	-637.1	FS	990.2	-899.2	N/A	N/A
	± 2%	1030.2	-1018.8		1159.1	-1291.0		
	± 3%	1098.0	-1029.0		1329.0	-1340.0		
2-PD	± 1%	672.4	-628.2	S	834.2	-683.9	2352.7	S
	± 2%	1051.2	-981.8		1296.3	-1212.6	1610.6	
	± 3%	1057.6	-945.2		1474.3	-1409.2	1188.6	
3-C	± 1%	568.6	-484.3	FS	761.2	-623.3	N/A	N/A
	± 2%	671.8	-629.1		835.4	-951.7		
	± 3%	681.7	-648.3		832.7	-982.2		
3-PD	± 1%	536.7	-536.5	FS	746.4	-710.4	2087.9	F
	± 2%	775.8	-740.8		914.9	-980.3	1984.4	
	± 3%	815.4	-775.2		981.3	-1198.7	1400.9	

The analysis showed that the finite element modeling overestimated the lateral force obtained from the laboratory test result. Furthermore, it was also found that the specimens with partial diagonal reinforcement dissipated more energy compared to those with a conventional layout. Spec. 2-PD dissipated 2.2% more energy compared to Spec. 2-C. Meanwhile, Spec. 3-PD dissipated 12.4% more energy compared to Spec. 2-C.

3.2 Comparisons of Crack Patterns

Comparisons of crack patterns for each specimen at a drift ratio of 3% are presented in Figure 7. In ANSYS' notation, a horizontal line represents a flexural crack, an inclined line represents a shear crack, and a hexagonal represents crushing of the concrete.

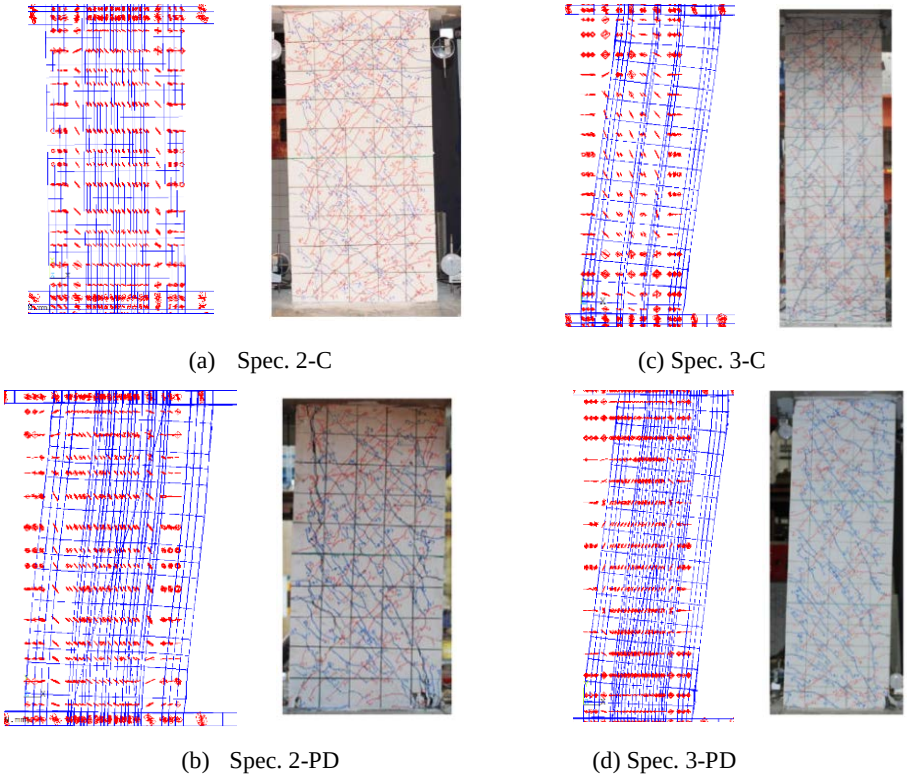

(a) Spec. 2-C (c) Spec. 3-C

(b) Spec. 2-PD (d) Spec. 3-PD

Figure 7 Comparisons of crack patterns at a drift ratio of 3%.

The crack patterns of Spec. 2-C (Figure 7(a)) indicate that crushing of the concrete occurred at the beam end. Similar observations were also made for Spec. 2-PD (Figure 7(b)). Meanwhile, the crack patterns of Spec. 3-C (Figure

7c) show that some tensile cracking occurred at mid-span of the beam, followed by crushing of the concrete at the beam ends. The crack patterns of Spec. 3-PD (Figure 7(d)) are similar to those of Spec. 3-C. It is worth noting that more cracks resulted in the specimens with diagonal reinforcement. This may imply that more energy is dissipated in these specimens as suggested by the cumulative energy dissipation presented in the hysteretic loops. Details on this calculation can be found elsewhere [12].

3.3 Estimation of Shear Strength Contributed by Concrete

In the current ACI 318-14 design approach for coupling beams with diagonal reinforcement, the ACI 318 design equation simply neglects the shear strength contributed by the concrete and assigns all shear demand to be resisted by the diagonal bars, as shown in Eq. (1). As has been explained previously, by including the concrete contribution, the number of diagonal bars can be reduced and results in a so-called partial diagonal layout as used in Spec. 2-PD and Spec. 3-PD in this study. Hence, it is of interest to evaluate the amount of shear strength contributed by both the concrete and the diagonal bars independently for these two specimens.

In this study, the total shear strength of a coupling beam, $V_{n,proposed}$ is given by Eq. (2),

$$V_{n,\text{proposed}} = V_{c,\text{ANSYS}} + V_d \tag{2}$$

The shear strength contribution of diagonal bars V_d shown in the second term is evaluated similar to Eq. (1), while the concrete contribution, $V_{c,ANSYS}$ is evaluated along a 45° inclined plane at the beam end using ANSYS:

$$V_{\text{c,ANSYS}} = \overline{\tau_{x1y1}} \times L \times b \times \sin\theta \tag{3}$$

where $\overline{\tau_{x1y1}}$ is the average shear stress evaluated along crack length L, b is the width of the coupling beam, and θ is the crack angle and can be taken as 45°. The crack angle of 45° is consistent with the crack angle observed during testing, as shown in Figure 7. Meanwhile, the crack length (L) can be simply calculated as h/sin45°, where h is the beam depth, taken as 500 mm. Using the aforementioned equations, the shear strength is then calculated at three different drift ratios, i.e. 1%, 2%, and 3%, as shown in Table 3.

Table 3 shows that as the drift ratio increases, the contribution of the concrete diminishes. This phenomenon can be understood because more cracks are developed at larger drift ratios. Secondly, at a drift ratio of 3%, the calculated shear strength ($V_{n,proposed}$) for specimen 2-PD was 1188.6 kN, while the maximum lateral force obtained from the hysteretic loop was 1409 kN. This

implies that this specimen should have failed in shear as indicated in the last column of Table 2. This finding is actually consistent with test results reported elsewhere [10]. Meanwhile, at a DR of 3%, the calculated $V_{n,proposed}$ for Spec. 3-PD was 1400.9 kN, while the maximum lateral force obtained from the hysteretic loop was 1198.7 kN. This suggests that the failure of this specimen should be governed by its flexural behavior, as presented in the last column of Table 2, and agrees with test results reported elsewhere [10].

Table 3 Shear strength evaluation.

Spec.	DR	τ_{x1y1} [MPa]	L [mm]	b [mm]	fy [MPa]	A_{vd} [mm^2]	α [deg]	$V_{c,ANSYS}$ [kN]	V_d [kN]	$V_{n,proposed}$ [kN]
2-PD	1%	17.1	707	300	487	981.7	12.0	2153.9	198.8	2352.7
	2%	11.2						1411.8		1610.6
	3%	7.9						989.8		1188.6
3-PD	1%	16.2	711.7	300	466	981.7	8.8	1949.4	138.5	2087.9
	2%	15.3						1845.9		1984.4
	3%	10.5						1262.4		1400.9

Thirdly, the accuracy of the calculated shear strength can only be verified if the specimen fails in shear. If the specimen fails in flexure, then the calculated shear strength is only hypothetical and can only serve as a value to justify qualitatively the failure mode of that particular specimen. Hence, in this study, only Spec. 2-PD failing in shear can be used to evaluate the accuracy of the predicted shear strength. Table 2 suggests that the maximum lateral force obtained from the test result was 1057.6 kN, while the predicted shear strength ($V_{n,proposed}$) was 1188.6 kN. From this specimen alone, the calculated shear strength is accurate, although more study is needed.

4 Conclusions

This study found some discrepancies that occurred between the hysteretic loops obtained from the test results and those obtained from the finite element analysis. The hysteretic loops obtained from finite element analysis tended to overestimate the lateral force. The finite element analysis could provide shear strength estimations contributed by both concrete and diagonal bars. Verifications with two specimens with partial diagonal layout showed good agreement between the shear strength estimated by the finite element analysis and that of the test results. Finally, the finite element analysis suggested that the contribution of the concrete to the total shear strength is crucial. Further research is needed to conclusively endorse this phenomenon in the design equation.

References

[1] ACI 318-14, *Building Code Requirement for Structural Concrete (ACI 318-14) and Commentary (ACI 318R-14)*, American Concrete Institute, 2014.

[2] ASCE/SEI 41-17, *Seismic Evaluation and Retrofit of Existing Buildings*, American Society of Civil Engineers, 2017.

[3] Lim, E., Hwang, S.J., Wang, T.W. & Chang, Y.H., *An Investigation on the Seismic Behavior of Deep Reinforced Concrete Coupling Beams*, ACI Structural Journal, **113**(2), pp. 217-226, 2016.

[4] Lim, E., Hwang, S.J., Cheng, C.H. & Lin, P.Y., *Cyclic Tests of RC Coupling Beam with Intermediate Span-to-Depth Ratio*, ACI Structural Journal, **113**(3), pp. 515-524, 2016.

[5] Lim, W.Y, Kang, T. H.K. & Hong, S.G., *Effect of Reinforcement Details on Seismic Precast Concrete Wall-Steel Coupling Beam Systems*, ACI Structural Journal, **115** (6), pp. 1751-1764, 2018

[6] Choi, Y, Hajyalikhani, P. & Chao, S.H., *Seismic Performance of Innovative Reinforced Concrete Coupling Beams – Double-Beam Coupling Beam*, ACI Structural Journal, **115**(1), pp. 113-125, 2018.

[7] Fisher, A.W., Bentz, E.C. & Collins, M.P., *Response of Heavily Reinforced High-Strength Concrete Coupling Beams*, ACI Structural Journal, **114**(6), pp. 1483-1494, 2017.

[8] Budiono, B., Nurjannah, S.A. & Imran, I., *Non-linear Numerical Modeling of Partially Pre-Stressed Beam-column Sub-Assemblages Made of Reactive Powder Concrete*, Journal of Engineering and Technological Sciences, **51**(1), pp. 28-47, 2019.

[9] Gunadi, R., Budiono, B., Imran, I. & Sofwan, A., *The Behavior of Slab-Column Connections with Modified Shear Reinforcement under Cyclic Load*, Journal of Engineering and Technological Sciences, **46**(1), pp. 17-36, 2014.

[10] Lim, E., *Cyclic Shear Strength and Seismic Design of Reinforced Concrete Coupling Beams*, PhD Dissertation, Dept. of Civil Engineering, National Taiwan University, Taipei, Taiwan, 2015.

[11] ACI 374.1-05, *Acceptance Criteria for Moment Frames Based on Structural Testing (ACI 374.1-05)*, American Concrete Institute, 2005.

[12] Dewi, N.T.H., *Shear Strength Analysis of Reinforced Concrete Coupling Beams Considering Concrete Contribution for Various Span-to-Depth*, Master Thesis, Dept. of Civil Engineering, Institut Teknologi Bandung, Bandung, 2017. (Text in Indonesian)